Inorganic Chemistry

Article

pubs.acs.org/IC

Coordination-Induced Spin-State Change in Manganese(V) Complexes: The Electronic Structure of Manganese(V) Nitrides

Henning Kropp,[†] Andreas Scheurer,[†] Frank W. Heinemann,[†] Jesper Bendix,[‡] and Karsten Meyer*[,†]

[†]Department of Chemistry and Pharmacy, Inorganic Chemistry, Friedrich-Alexander University Erlangen-Nürnberg (FAU), Egerlandstrasse 1, 91058 Erlangen, Germany

[‡]Department of Chemistry, University of Copenhagen, Universitetsparken 5, DK-2100 Copenhagen, Denmark

Supporting Information

ABSTRACT: This work illustrates that manganese(V) nitrido complexes are able to undergo a coordination-induced spin-state change by altering the ligand field from trigonal to tetragonal symmetry. For the reversible coordination of acetonitrile to trigonal $[(TIMEN^{xyl})Mn(N)]^{2+}$ (**1**; high-spin $S = 1$; with $TIMEN^{xyl}$ = tris[2-(3-xylylimidazol-2-ylidene)ethyl]-amine), a temperature-dependent coordination-induced spin-state switch is established. Starting from the manganese(V) nitrido complex **1**, the synthesis and characterization of a series of octahedral, low-spin ($S = 0$) manganese(V) nitrido complexes of the type $[(TIMEN^{xyl})Mn(N)(L)]^{n+}$ (L = MeCN (**2**), ^{t}BuNC (**3**), CN^{-} (**4**), NCS^{-} (**5**), F^{-} (**6**), μ-$\{Ag(CN)_2\}^{-}$ (**7**), with $n = 1, 2$) is described. These represent the first examples of d^2 transition metal complexes showing a coordination-induced spin-state change. Spectroscopic, as well as ligand-field theory and density functional theory studies suggest a transition from a 2 + 2 + 1 orbital splitting in the trigonal case to a 1 + 2 + 1 + 1 splitting in tetragonal symmetry as the origin of the coordination-induced spin-state change.

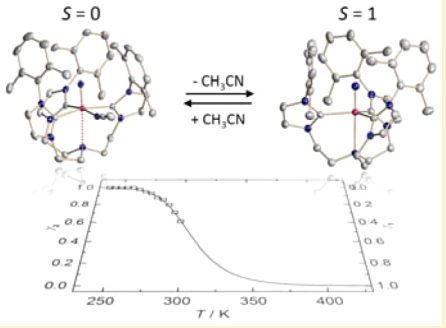

INTRODUCTION

For transition metal complexes the term spin crossover (SCO) refers to the ability of the metal center to undergo a spin transition in response to external stimuli. In most cases, magnetic bistability is the origin of this phenomenon.[1−7] It is generally accepted that the SCO effect is limited to 3d transition metal ions with a d^4−d^7 electron configuration.[2,8−10] Most known SCO complexes possess iron(II),[2,11−35] iron(III),[2,36−45] and cobalt(II)[46−48] metal centers. Few examples with manganese(II), manganese(III), chromium(II),[2,49] and cobalt(III) ions,[47,50−53] as well as spin-state equilibria for nickel(II)[2,54−56] complexes in solution, exist. The latter are the only examples for $3d^8$ SCO systems. For all of these examples, changes of the magnetic properties are accompanied by structural changes of the complex geometry.[9] To the best of our knowledge, SCO behavior has never been described for high-valent transition metal complexes with a d electron count smaller than d^4.

Recently, Thies et al. described a coordination-induced spin crossover (CISCO) in solution for nickel(II) porphyrin complexes by axial coordination of pyridine derivatives.[57] Later, the authors introduced the light-driven coordination-induced spin-state switch (LD-CISSS), a special case of CISCO, by utilizing the light-induced *cis*−*trans* isomerism of azopyridines to switch between square-planar (low-spin, $S = 0$) and octahedral (high-spin, $S = 1$) coordination of the nickel(II) porphyrin in solution at room temperature.[58−62] To expand the CISCO concept, we set out to identify other examples beyond the range of Ni(II) porphyrin complexes and the known d^4−d^7 systems. Generally, the electronic structure of d^2 first row transition metal complexes with strong π-donor ligands, such as nitrido ligands, is strongly dependent on the geometry of the ligand sphere.[63−67] The majority of these molecular nitride complexes possesses tetragonal symmetry and thus have a nonmagnetic singlet ground state.[68−81] A trigonal symmetry around the metal center instead leads to a triplet ($S = 1$) ground state (see Figure 1).[82]

Recently, we reported the synthesis and characterization of a series of trigonal Mn nitride complexes in oxidation states +3, +4, and +5, including the first paramagnetic ($S = 1$) manganese(V) nitride, namely, $[(TIMEN^{xyl})Mn(N)](PF_6)_2$ (**1**) (with $TIMEN^{xyl}$ = tris[2-(3-(2,6-xylyl)imidazol-2-ylidene)-ethyl]amine). This complex—a well-defined C_3-symmetric d^2 system—is a sensitive probe for the influence of complex geometry on the electronic structure. The five-coordinate Mn^{V} ion in **1** is situated in a sterically demanding, trigonal bipyramidal ligand environment, with the $Mn^{V}{\equiv}N$ moiety located in a tight cylindrical cavity formed by the three xylyl substituents of the tetradentate $TIMEN^{xyl}$ ligand.[82] However, the $TIMEN^{xyl}$ ligand has proven to be moderately flexible and to allow for metal coordination numbers higher than five, as shown in the six-coordinate cobalt(III) peroxo complex $[(TIMEN^{xyl})Co(O_2)]BPh_4$.[83] Therefore, the coordinatively unsaturated manganese(V) center in **1** was expected to perform a spin-state change, by transition from trigonal to tetragonal

Received: January 21, 2015
Published: March 26, 2015

DOI: 10.1021/acs.inorgchem.5b00112
Inorg. Chem. 2015, 54, 3562−3572

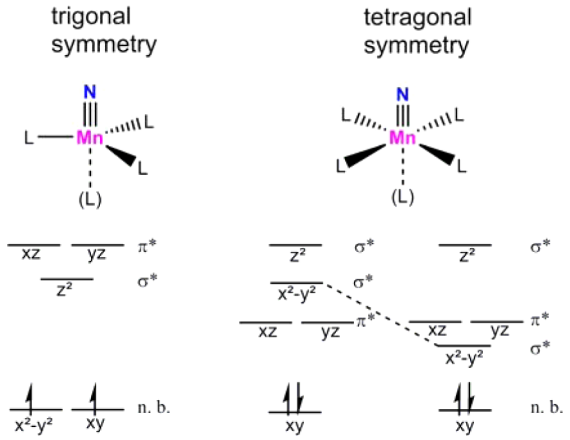

Figure 1. Qualitative d-orbital splitting diagrams for Mn^{V} nitrido complexes in trigonal (left) and tetragonal (right) ligand fields. For the tetragonal complexes the relative position of the $d(x^2-y^2)$ orbital depends on the strength of the equatorial ligand field (dotted line).

symmetry upon coordination of an additional equatorial ligand L (Scheme 1).

Similar to the known CISCO, the first example of a d^2 transition metal complex showing a coordination-induced spin-state change is presented here. The reversible temperature-dependent coordination-induced spin-state-switch (TD-CISSS) of **1** in acetonitrile, as well as an irreversible spin-state change by coordination of additional ligands, is described as well. We employed the electrophilicity of the high-valent manganese(V) center in **1** to prepare a series of tetragonal manganese(V) nitride complexes of the type $[(TIMEN^{xyl})Mn(N)(L)]^{n+}$ (L = MeCN, ^{t}BuNC, CN^-, NCS^-, F^-, μ-$\{Ag(CN)_2\}^-$; with n = 1, 2) and carried out spectroscopic, as well as theoretical studies, to compare those nonmagnetic (S = 0) complexes with the paramagnetic, high-spin (S = 1), trigonal analogue **1**.

Scheme 1. Spin-State Change in Mn^{V} Nitride Complexes

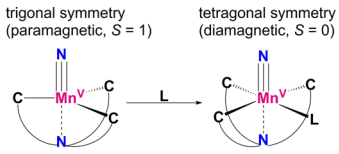

L = MeCN (**2**), ^{t}BuNC (**3**), CN^- (**4**), NCS^- (**5**), F^- (**6**), μ-$\{Ag(CN)_2\}^-$ (**7**)

RESULTS AND DISCUSSION

Synthesis and Spectroscopic Studies. When a solution of **1** in acetonitrile is stored in the freezer at −35 °C for several minutes an obvious color change from brown-orange to purple occurs, hinting at a significant change in ligand field (LF) strength and a possible change of the spin-state in complex **1** (Scheme 2). Therefore, we followed the temperature-related electronic structure changes of **1** by variable-temperature (VT) UV−vis spectroscopy (Figure 2). The temperature-dependent color change in acetonitrile can be explained by a TD-CISSS (Scheme 2). The low-temperature spectrum features three absorption bands centered at λ = 327, 402, and 542 nm (with a relative ratio of absorbance of 100:18:15). A possible coordination of acetonitrile in the equatorial plane of the trigonal, paramagnetic (d^2, S = 1) manganese(V) center in **1** at low temperatures would result in the formation of the

Scheme 2. Temperature-Dependent Coordination of Acetonitrile to 1 Resulting in a TD-CISSS

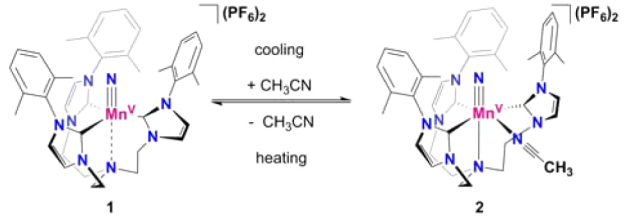

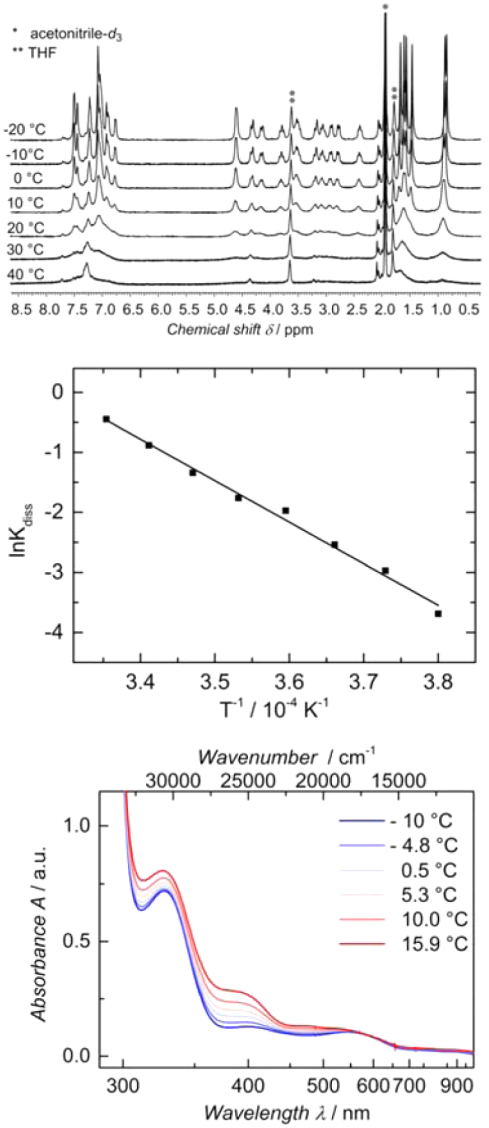

Figure 2. TD-CISSS behavior of **1** in acetonitrile. (upper) VT ^{1}H NMR spectrum of **1** in acetonitrile-d_3 in the temperature range from −20 to 40 °C. (center) Van't Hoff plot for the dissociation of the equatorial acetonitrile ligand from **2**. ΔH_{diss} = +57.5 ± 0.5 kJ mol^{-1} ΔS_{diss} = +0.2 kJ mol^{-1} K^{-1}. (lower) VT UV−vis spectrum of **1** in a solution of acetonitrile.

tetragonal, diamagnetic (d^2, S = 0) species $[(TIMEN^{xyl})Mn(N)(NCMe)]^{2+}$ (**2**).

Since **1** is NMR silent, it should conveniently be possible to follow the formation of **2** by VT ^{1}H NMR. Thus, when a solution of **1** in acetonitrile-d_3 is cooled below 0 °C inside the NMR spectrometer, the appearance of more than 20 signals of

DOI: 10.1021/acs.inorgchem.5b00112
Inorg. Chem. 2015, 54, 3562−3572

2 in the diamagnetic chemical shift range for protons can be observed (Figure 2). In **2**, each of the six methyl groups of the $TIMEN^{xyl}$ ligand appears as a sharp singlet in the diamagnetic range between 1.7 and 0.8 ppm and can unambiguously be identified by integration. Similarly, the 12 protons of the ethylene bridges give rise to 10 signals between 4.6 and 2.4 ppm. Integration reveals that two of these signals originate from four accidentally isochronous proton resonances. The aromatic region is not well-resolved, and the signals in this region cannot be assigned. The low-temperature ^{13}C NMR spectrum shows one signal for each of the 39 carbon atoms of the $TIMEN^{xyl}$ ligand (see Experimental Section for detailed description of the spectrum). Signals for the coordinated acetonitrile cannot be observed, which is likely due to superimposition and low concentration compared to the deuterated solvent signals.

To investigate the temperature dependence of the equilibrium between paramagnetic **1** and diamagnetic **2**, a VT ^1H NMR experiment was conducted. Unfortunately, decomposition of complexes **1** and **2** was observed in solution at temperatures above +40 °C, which restricted the temperature range of investigation from −40 to +40 °C. In this interval, ^1H NMR spectroscopy revealed the interconversion from **1** to **2** as fully reversible. However, substantial broadening of the signals, induced by the growing fraction of paramagnetic **1**, was observed at temperatures higher than +25 °C. Therefore, and only in the temperature range from −40 to +25 °C, integration of two methyl resonances, stemming from the xylyl groups at ~0.8 ppm, allowed for accurate determination of the molar fractions γ_2 and γ_1, respectively (hexamethyldisiloxane was used as internal integration standard; Figure 3). In addition, it was

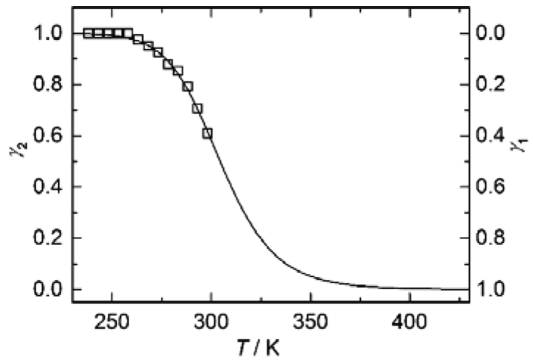

Figure 3. Temperature-dependence of the molar fraction γ_2 and γ_1 of the low-spin species **2** and the high-spin species **1**, obtained by integration of the ^1H NMR spectrum (black squares). The black line represents a fit of the experimental data based on the Van't Hoff equation.

shown that the equilibrium is completely shifted to **2** at temperatures lower than −10 °C. From this collected data set, the dissociation enthalpy ΔH_{diss} of the equatorially coordinated acetonitrile ligand was determined to be 57.5 ± 0.5 kJ mol^{-1} (Figure 2), while the corresponding entropy ΔS_{diss} is +0.2 kJ mol^{-1} K^{-1}.

To gain deeper insight into the properties of this system and to verify the hypothesis of a TD-CISSS due to acetonitrile coordination, we sought to synthesize a series of tetragonal Mn^V nitride complexes starting from trigonal **1**. Considering the dissociation enthalpy of the acetonitrile ligand in **2**, strong donor ligands are necessary to obtain stable, tetragonal analogues of **2**. Therefore, a series of ligands ranging from good π-acceptors, like CN^-, to the pure donor ligand F^-, spanning nearly the whole range of the spectrochemical series, was chosen. Addition of ^{t}BuNC to a brown-orange solution of $[(TIMEN^{xyl})Mn(N)](BPh_4)_2$ results in the formation of the pale pink complex $[(TIMEN^{xyl})Mn(N)(CN^tBu)](BPh_4)_2$ (**3**), while treatment with tetrabutylammonium cyanide or sodium thiocyanate yields the corresponding cyano and iso-thiocyanato complexes isolated as $[(TIMEN^{xyl})Mn(N)(CN)]BPh_4$ (**4**) and $[(TIMEN^{xyl})Mn(N)(NCS)]BPh_4$ (**5**), respectively. While oxidation of the Mn^{IV} nitride complex $[(TIMEN^{xyl})Mn(N)]BPh_4$ with AgF furnishes the corresponding fluoride analogue $[(TIMEN^{xyl})Mn(N)(F)]BPh_4$ (**6**), treatment of the Mn^{IV} precursor with AgCN does not afford **4**, but leads to the formation of the dicyanoargentate-bridged dimer $[\{(TIMEN^{xyl})Mn(N)\}_2\mu\text{-}\{Ag(CN)_2\}](BPh_4)_3$ (**7**). Although bulk isolation of pure samples of the dinuclear manganese(V) complex **7** was not accomplished, diffusion of benzene into the crude reaction mixture yielded single crystals of **7** suitable for X-ray diffraction studies and a pink amorphous solid.

The electronic absorption spectra of compounds **3**−**6** (Figure 4, Table 1) in acetonitrile are consistent with the

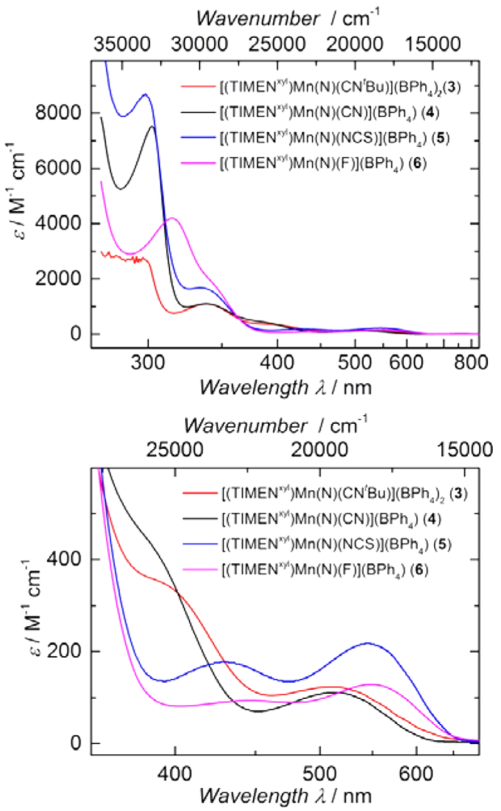

Figure 4. Electronic absorption spectra of **3**−**6**, recorded in acetonitrile solution (for **1** and **2**, see Figure 2).

low-temperature spectrum of **1** in acetonitrile solution, which gives evidence for the suggested spin-state change in the equilibrium **1** ⇌ **2**. All spectra feature an absorption band of low intensity (ε = 110−218 M^{-1} cm^{-1}) in the region of λ = 510−550 nm and a second weak transition (ε = 92−438 M^{-1} cm^{-1}) in the range of λ = 385−453 nm. For complexes **5** and **6**, the lowest energy absorption at λ_{max} > 500 nm is more intense than the one at ~440 nm. For complexes **3** and **4**, this intensity pattern appears to be reversed, but the Gaussian deconvolution reveals this to be mainly due to intensity from the higher-

DOI: 10.1021/acs.inorgchem.5b00112
Inorg. Chem. 2015, 54, 3562−3572

Table 1. Absorption Maxima and Corresponding Extinction Coefficients of Complexes 3−6 in Acetonitrile[a]

	λ_{max} [nm] (ε [M^{-1} cm^{-1}])			
		d(xy) → 3d(z^2)/ 4p(z)	d(xy) → d(x^2-y^2)	d(xy) → {d(xz),d(yz)}
3		338 (1094)	393 (351)	510 (123)
			24 840/2560	19 910/4600
4	302 (7517)	338 (1100)	385 (438)	513 (110)
			25 410/2740	19 750/4040
5	298 (8677)	333 (1676)	430 (178)	545 (218)
			23 380/5050	18 170/2840
6	315 (4195)	343 (1873)	453 (92)	550 (145)
			22 050/6280	17 930/2500

[a]The second row gives the parameters of the Gaussian deconvolution (Figures S15−S19, Supporting Information) of the low-energy part of the spectrum (ν_{max} [cm^{-1}]/fwhh [cm^{-1}]).

energy transitions overlapping with the bands located at $\lambda \approx$ 390 nm. A third absorption band of considerable higher intensity (ε = 1094−1873 M^{-1} cm^{-1}), centered at $\lambda \approx$ 340 nm, is observed for all complexes. For **4**−**6**, another high intensity absorption (ε = 4195−8677 M^{-1} cm^{-1}) is centered at $\lambda \approx$ 300 nm. For compound **3**, this transition is likely blue-shifted into the broad and intense absorptions in the UV region and hence, cannot be observed. Note that for compounds **3** and **4** the position of the lowest-energy band is very close to that of $[Mn(N)(CN)_5]^{3-}$ (λ_{max} = 516 nm), and, as this is the only band in the visible range, these compounds have a similar pink-purple color.[84]

In the ^{1}H NMR spectra, complexes **3**−**6** all show well-resolved signals in the diamagnetic region, reminiscent of **2**. Coordination of the equatorial ligand L removes the C_3 symmetry of precursor **1**, resulting in one proton resonance for each of the methyl groups as well as for all other remaining protons of the TIMEN^{xyl} ligand. In addition, one characteristic feature in all complexes **3**−**6** is that, for the four-spin system of one of the three ethylene bridges (established by combination of ^{1}H, ^{1}H−^{1}H COSY, ^{13}C, and ^{1}H−^{13}C HMQC spectra), four well-resolved doublet of doublets were recorded. This coupling pattern is persistent at increased temperatures. Interestingly, the spectroscopic data imply a vicinal coupling constant of $J \approx$ 0 Hz. Following the correlation of torsion angle Φ and vicinal coupling constants resulting from the Karplus curve,[85−87] $J \approx 0$ Hz leads to torsion angles Φ of ∼80−100° in complexes **3**−**6**. This piece of spectroscopic evidence implies a very similar arrangement of the ethylene bridges in the N-anchor moiety in all complexes **3**−**6** in solution as well as in the solid state (see crystallographic data). Furthermore, the loss of symmetry is also reflected in the ^{13}C NMR spectra of **3**−**6**, where each carbon atom of the TIMEN^{xyl} ligand produces one signal.

Superconducting quantum interference device (SQUID) magnetization measurements reproducibly present temperature-independent, negative molecular susceptibilities, thus confirming the diamagnetism of the described tetragonal Mn^V nitride complexes (d^2, low-spin, S = 0). Temperature-independent paramagnetism (TIP), as present in manganese(V) nitride complexes bearing the cyclam ligand,[77] was not observed.

In complexes **2**−**5** and **7**, the additional ligand L coordinates via its C≡N entity to the metal center, which provides a convenient probe to study the binding mode of the ligand by IR vibrational spectroscopy. Table 2 summarizes the vibrational

Table 2. CN Stretching Vibrations ($\tilde{\nu}_{obs}$) for Compounds 3−5 and 7 (in KBr) Compared to the Free Ligands L ($\tilde{\nu}_{free}$) and the Shift in Frequency ($\Delta\tilde{\nu}$) in cm^{-1}

	3	**4**	**5**	**7**
$\tilde{\nu}_{obs}$	2185	2120	2085	2185
$\tilde{\nu}_{free}$	2136[a]	2077[b]	2046[c]	2140[d]
$\Delta\tilde{\nu}$	+49	+43	+39	+45

[a]*tert*-butyl isocyanide, liquid film.[88] [b]KCN, nujol mull.[88] [c]KSCN, nujol mull.[88] [d]K[Ag(CN)$_2$], nujol mull.[89]

frequencies of the CN stretch in complexes **3**−**5** and **7**. For all complexes, the vibration is blue-shifted by 39−49 cm^{-1} compared to that of free L = ^{t}BuNC, CN^-, NCS^-, and μ-$\{Ag(CN)_2\}^-$,[88,89] which is indicative of a predominant M−L σ interaction. This "non-classical" behavior has already been described for a series of main group[90−96] and transition metal compounds.[97−102] However, the shift toward higher wavenumbers of the CN stretching frequencies in σ-only binding isocyanides is reported to be significantly higher (73−94 cm^{-1})[103,104] than the shift observed for complexes **3**−**5** and **7**. La Pierre et al. recently showed that a blue shift of ∼40−50 cm^{-1} for coordinated isocyanides is due to mainly σ binding with a small contribution of π-backbonding.[105] The shift in the CN stretching frequency of the ^{t}BuNC, CN^-, NCS^-, and μ-$\{Ag(CN)_2\}^-$ derivatives **3**−**5** and **7** falls exactly in that range, thereby suggesting some extent of π-backbonding to be present. Two possible origins of the π-backbonding must be considered: (1) The two remaining d electrons of the Mn^V center populate the metal-based d(xy) orbital that has suitable symmetry for π-backbonding into at least one of the π^*-orbitals of the equatorial ligand. This orbital is nonbonding with respect to the Mn^V≡N bond and thus should be available to provide the necessary electron density for weak π-backbonding. (2) The metal−nitride bonding orbitals of π-symmetry might be able to donate enough electron density into the π^*-orbitals of the CN moiety (by direct overlap of the corresponding orbitals) to cause weak π-backbonding. This binding mode has recently been reported for cationic vanadium(V) bis(imido) complexes with nitrile and isocyanide ligands.[105] Such a synergy between strong π-donor ligands and π-acceptor ligands has also been invoked to explain the stability of *trans*-dioxo complexes of molybdenum(IV) and tungsten(IV) with auxiliary phosphine and carbon monoxide ligands.[106] Unfortunately, the ν(Mn≡N) stretching frequencies, which could be helpful in distinguishing between both cases, could not be identified for complexes **3**−**7**, since they are obscured by ligand absorptions.

X-ray Crystallography. Single crystals suitable for X-ray diffraction analysis of tetragonal complexes **2**−**7** could be obtained (Figure 5). Selected bond lengths and angles of complexes **2**−**7** are given in Table 3, including the metric parameters of the previously published complex **1** for comparison.

In complexes of the type $[(TIMEN^{xyl})Mn(N)(L)]^{n+}$ (L = MeCN (**2**), ^{t}BuNC (**3**), CN^- (**4**), NCS^- (**5**), F^- (**6**), μ-$\{Ag(CN)_2\}^-$ (**7**), and n = 1, 2) the ligand L coordinates in the equatorial plane, thereby breaking the perfect C_3 symmetry of the trigonal bipyramidal complex **1**. The N_{anchor}−Mn≡N axis of **1** lies on a crystallographic C_3 axis, thus rendering all ∠C−Mn−C angles close to 120° and the ∠N_{anchor}−Mn≡N angle to be 180°. In contrast, and as a consequence of the equatorially bound L, the ∠C−Mn−C angles of the NHC chelator are changed drastically. In complexes **2**−**7** the metal center is

DOI: 10.1021/acs.inorgchem.5b00112
Inorg. Chem. 2015, 54, 3562−3572

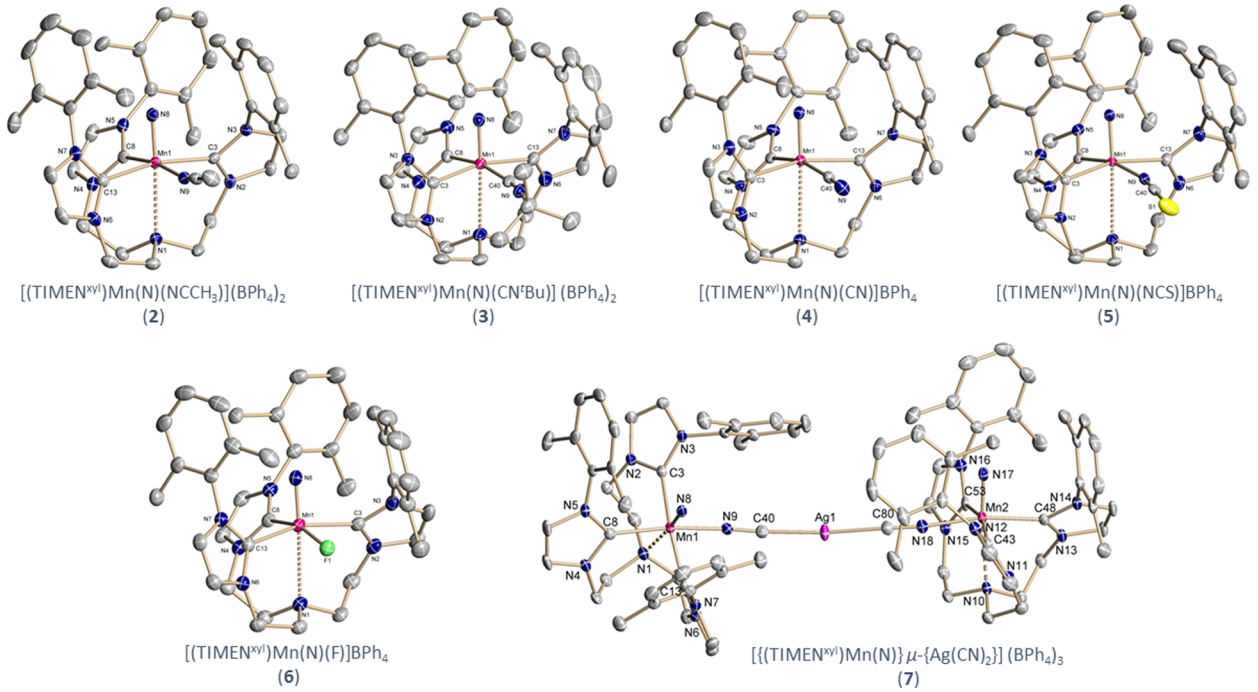

Figure 5. Molecular structures of the complexes **2**−**7** in crystals of **2**·MeCN, **3**·MeCN·1.25Et_2O, **4**·DME, **5**·Et_2O, **6**·2Et_2O, and **7**·2C_6H_6·0.125 MeCN. Solvent molecules, BPh_4^- counteranions, and hydrogen atoms are omitted for clarity; thermal ellipsoids are shown at 50% probability.

Table 3. Selected Bond Lengths [Å] and Angles [deg] for Compounds 1−7 from XRD Structure Analysis

	Mn≡N	Mn−N	Mn−C (average)	Mn−L	d(Mn_{doop})	C−Mn−C	C−Mn−L	N−Mn≡N	C−Mn≡N	L−Mn≡N
1[a]	1.546(3)	2.448(3)	2.054(2)		0.150	119.47(16)		180	94.19(6)	
						94.62(7)	80.58(6)		92.69(8)	
2	1.525(2)	2.482(2)	2.045(2)	2.030(2)	0.181	95.30(7)	87.97(6)	174.87(7)	93.86(7)	95.81(7)
						165.10(7)	170.93(7)		96.74(8)	
						92.76(11)	78.63(11)		94.30(11)	
3	1.520(2)	2.497(2)	2.058(3)	2.001(3)	0.208	95.67(10)	90.96(11)	176.03(1)	94.32(12)	95.40(11)
						164.88(11)	169.32(11)		97.52(11)	
						94.64(7)	77.31(7)		94.68(8)	
4	1.529(2)	2.573(2)	2.064(2)	1.994(2)	0.209	100.18(7)	85.20(7)	176.01	94.73(8)	98.69(8)
						160.10(7)	166.60(7)		97.19(8)	
						92.30(9)	79.35(8)		92.60(9)	
5	1.521(2)	2.602(2)	2.043(2)	2.030(2)	0.233	97.62(8)	87.69(8)	173.30	95.54(9)	100.71(9)
						162.55(9)	166.62(8)		98.30(9)	
						95.45(10)	79.32(8)		92.77(11)	
6	1.524(2)	2.616(2)	2.038(3)	1.909(2)	0.244	97.81(10)	83.29(9)	172.78	96.41(11)	105.18(9)
						159.61(10)	162.04(9)		98.34(11)	
						93.40(8)	79.95(8)		93.23(9)	
						95.03(8)	89.87(8)		94.82(9)	
7[b]	1.528(2)	2.504(2)	2.051(2)	2.003(2)	0.198	164.76(8)	170.67(7)	174.52	97.36(9)	95.20(8)
	1.523(2)	2.517(2)	2.058(2)	2.001(2)	0.210	93.13(8)	81.38(8)	174.05	93.41(9)	97.93(9)
						96.30(8)	87.01(8)		94.60(9)	
						164.68(8)	168.62(7)		96.85(9)	

[a]Taken from ref 82. [b]Values for both monomeric units are given.

coordinated octahedrally by the equatorial ligand L, the three N-heterocyclic carbene (NHC) carbon atoms, the nitrido ligand as well as the nitrogen anchor of the chelator. The Mn−N_{anchor} distances vary slightly depending on the nature of the equatorial ligand L and decrease along the series L = F^- (**6**) > NCS^- (**5**) > CN^- (**4**) > μ-$\{Ag(CN)_2\}^-$ (**7**) > ^{t}BuNC (**3**) > MeCN (**2**) from 2.616−2.482 Å. Obviously, the additional negative charge of the anionic ligands in **4**−**6** compensates for the electron deficiency of the highly oxidized Mn^V center, thus weakening the Mn−N_{anchor} interaction. In complexes **2** and **3**, carrying a neutral ligand L, the nitrogen anchor provides the additional electron density to stabilize the electron-deficient Mn^V center, resulting in stronger Mn−N_{anchor} interactions. Thus, in the absence of an equatorial ligand L the shortest Mn−N_{anchor} distance (2.448 Å) is observed for trigonal bipyramidal **1**. In **7**, only one negative charge is provided for

DOI: 10.1021/acs.inorgchem.5b00112
Inorg. Chem. 2015, 54, 3562−3572

two manganese centers, resulting in a Mn−N_{anchor} distance between that of **3** and **4**.

In the tetragonal Mn^V nitride complexes **2**−**7**, the metal nitride bond is significantly shortened (1.520−1.529 Å) compared to the trigonal nitride **1** (1.546 Å). The term "out-of-plane" (oop) shift has been coined for the distance of the manganese center from the plane, defined by the three carbene carbon atoms of the TIMEN ligand. The d(Mn_{oop}) is correlated to the Mn−N_{anchor} and the Mn≡N distance and increases slightly from trigonal (0.15 Å) to tetragonal symmetry (0.18−0.24 Å). Surprisingly, the nature of L has no significant effect on the Mn≡N bond length and the carbene bond trans to L. Although the changes in bond length by a small margin fulfill the 3σ rule, the average Mn−C_{TIMEN} bond distance in complexes **2**−**7** increases along the spectrochemical series for L = F^- (**6**) < NCS^- (**5**) < MeCN (**2**) < ^{t}BuNC (**3**) ≈ μ-{Ag(CN)$_2$}$^-$ (**7**) < CN^- (**4**). Compared to complex **1**, without an equatorial ligand L, the ∠N_{anchor}−Mn≡N angle is reduced in the tetragonal nitrido complexes **2**−**7** and ranges from 172.78° in **6** to 176.03°in **3**. This is mirrored in the ∠L−Mn≡N angle, which significantly differs from the ideal 90° and ranges from 95.4° in **3** to 105.18° in **6**. Since this effect is smallest in the ^{t}BuNC derivative **3**, and reaches its maximum in the case of the comparably small F^- ligand in **6**, it is implausible that steric interactions with the xylyl groups from the carbene ligand have any deciding importance. Instead, we note that optimizing the bond strength with the nitrido ligand favors ∠L−Mn≡N angles equal to the tetrahedral angle since this geometry removes the σ-overlap between the equatorial ligands and the metal d(z^2) orbital. Thus, angles significantly smaller than the tetrahedral angle might have sterically founded explanations (although d(z^2)−p(z) mixing also contributes). In all of the structures, short 1···5 contacts between a hydrogen from one of the ligand's methylene groups and the ligating atom of the ligand L are observed. All these contacts are shorter than the sum of the corresponding van der Waals radii (r_H = 1.06 Å, r_N = 1.46 Å, r_C = 1.53 Å, r_F = 1.40 Å).[107] Given that the ligand's ethylene groups ought to possess a significant degree of flexibility it is likely that these interactions are not sterically enforced.

The length of this contact varies, not surprisingly, opposite to the L−Mn≡N angle: 2.192 Å (**6**) < 2.366 Å (**5**) < 2.385/2.409 Å (**7**) < 2.421 Å (**2**) ≈ 2.425 Å (**3**) ≈ 2.430 Å (**4**). Notably, the C−H···F distance of 2.192 Å in **6** is significantly shorter (>0.2 Å) than similar interactions, which have been interpreted as C−H···F hydrogen bonding.[108] It is also revealing that the N-bonded cyanide in **7** allows a shorter interaction than all of the C-bonded ligands, including cyanide with its full negative charge. These observations support that steric and electronic interactions with the methylene group of one strand of the tripodal ligand are determining the variation of the L−Mn≡N angle for these systems.

Electronic Structure Considerations. For all systems, two bands are observed with intensities that unambiguously characterize them as spin-allowed LF transitions. The third band observed at $\lambda \approx 340$ nm has $\varepsilon > 1000$ M^{-1} cm^{-1}, and although its d−d character is less clear, it cannot be ruled out (vide infra). For the two spin-allowed bands there are two possible assignments: They may be assigned as components of the transition to the set of π^*-orbitals in tetragonal symmetry, d(xy) → {d(xz),d(yz)},[77,84] which is split by the lower symmetry of the equatorial LF. In this case, the d(xy) → d(x^2−y^2) must be high in energy and masked by charge-transfer and intraligand transitions. The d(xy) → d(x^2−y^2) transition cannot reasonably be assigned to the band at $\lambda \approx 340$ nm due to the approximately constant energy of this band among the systems (variation is less than 900 cm^{-1}). Furthermore, the high extinction coefficient is incommensurable with that excitation being orbitally forbidden in perfect tetragonal symmetry. The alternative assigns the two lowest energy bands as transitions to a not discernibly split {d(xz),d(yz)} set, followed by the d(xy) → d(x^2−y^2) transition at higher energy.

These alternatives are discussed below based on an additive LF model of the fluoride complex (**6**), as it is the one deviating the most from orthoaxial coordination and hence represents the system for which the geometric effects of low symmetry should be most pronounced. With only two experimental observations for each system, the angular overlap model (AOM) cannot circumvent an overparameterization. Even if parameter transferability is assumed for the nitrido ligand, the number of observations is insufficient to allow for determination of e_σ^L and e_π^L values as well as the parameters for the TIMEN^{xyl} ligand. The AOM-based expressions for the energies of the d orbitals are given in the Supporting Information (Figure S20, L is in the xz-plane). From these, the orbital energy differences follow as eqs 1−4:

$$E(x^2 - y^2) - E(xy) = 1.92e_\sigma^C + 0.65e_\sigma^L - 2.68e_\pi^C - 0.87e_\pi^L \quad (1)$$

$$E(xz) - E(xy) = e_\pi^N - 0.08e_\sigma^C + 0.19e_\sigma^L - 1.79e_\pi^C - 0.19e_\pi^L \quad (2)$$

$$E(yz) - E(xy) = e_\pi^N + 0.01e_\sigma^C - 1.00e_\pi^C - 0.86e_\pi^L \quad (3)$$

$$\Delta(E[C_{4v}]) = E(xz) - E(yz) = -0.09e_\sigma^C + 0.19e_\sigma^L - 0.79e_\pi^C + 0.67e_\pi^L \quad (4)$$

If the highest energy band (>20 000 cm^{-1}), which shows the largest variation in energy between the systems, is assigned to a transition into d(x^2−y^2), then the energy of this band should correlate positively with the σ-donor strength of the ligand L. This is clearly observed experimentally. If, conversely, the second band is assigned to a transition into a component of the {d(xz),d(yz)} set, then this component must be the one with higher sensitivity with respect to the e_π^L, which implies that d(yz) is highest in energy. Consequently, a situation where $e_\pi^L < e_\pi^C$ results, which certainly is improbable for well-established π-donor ligands F^- and NCS^-. If we consider the width of the lowest energy band, the Gaussian deconvolution clearly yields the broadest first bands for the π-acceptor ligands (^{t}BuNC, CN^-). The splitting of the {d(xz),d(yz)} set of orbitals is given directly by the difference $e_\pi^L - e_\pi^C$ for the orthoaxial system. However, the deviations from orthoaxiality have an interesting and important consequence for this splitting, which obtains the parametrical expression: $\Delta(E(C_{4v})) = (0.19e_\sigma^L - 0.09e_\sigma^C) + (0.67e_\pi^L - 0.79e_\pi^C)$. Since it is very conceivable that $e_\sigma^L < 2\ e_\sigma^C$ for the weaker ligands (F^-, NCS^-), the σ contributions to this splitting will tend to cancel out for these ligands, but not so for ligands that exhibit comparable σ-donor strength to the carbenes.

In accordance with this, the Gaussian deconvolution of the first band yields distinctly narrower bands for the weak-field ligands (F^-, NCS^-) as compared to the strong-field ligands (^{t}BuNC and CN^-). Furthermore, for the actual geometry of the

DOI: 10.1021/acs.inorgchem.5b00112
Inorg. Chem. 2015, 54, 3562−3572

fluoride complex, the π contribution to the splitting of the {d(xz),d(yz)} set is attenuated to be only ca. three-fourths of the value in the orthoaxial case, making it plausible that experimental observation of the splitting is difficult. Both of these observations support the assignment d(xy) → {d(xz),d(yz)} and d(xy) → d(x^2-y^2) based on the band positions. This assignment is also corroborated by ligand field theory (LFT) oriented density functional theory (DFT) calculations. Virtual Kohn–Sham orbital energies from DFT are normally poor representations of excited orbital energies in LFT modeling. Therefore, the so-called average-of-configuration (AOC) computation has been employed in mapping DFT calculations on LFT models.[109,110] This method has been shown to be reliable in extracting LF parameters from DFT computational results. Straightforward, closed-shell AOC calculations for models of the fluoride **6** (Figure 6) and the cyanide **4**

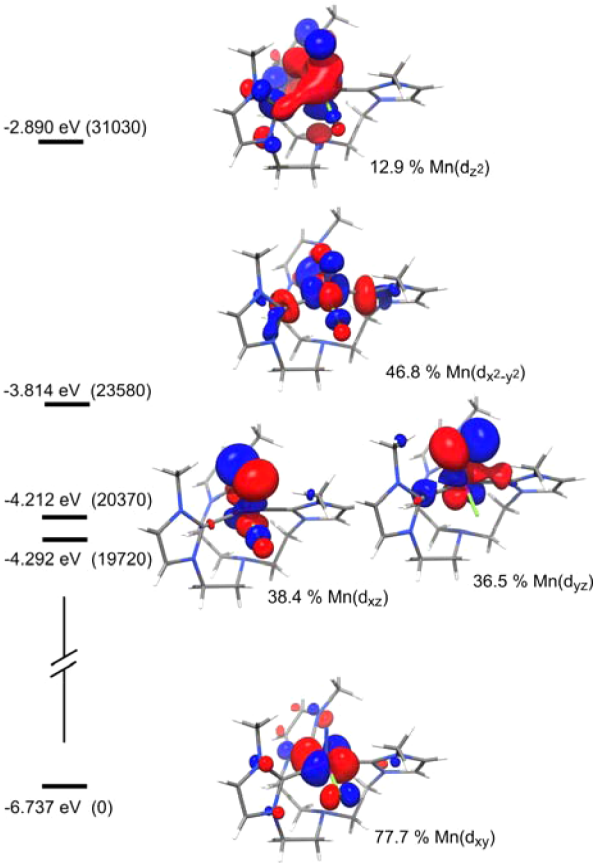

Figure 6. Orbital energy diagram for the five partially populated orbitals in the AOC computation (ADF, PBE0, TZV2P) on complex **6** with computed energies (eV) and relative energies (cm^{-1}, in parentheses). A common orientation has been used for all orbitals, though the Mn ($3d_{z^2}$) character of the highest lying orbital is more palpable in other projections (Figure S21, Supporting Information).

complexes, with methyl groups instead of xylyl groups, yield the d-orbital ordering d(xy) < {d(xz),d(yz)} < d(x^2-y^2) < d(z^2) in both cases. The splitting of the set {d(xz),d(yz)} is calculated to be less than 1000 cm^{-1}. Since the π-acceptor character of NHC's with transition metals has been debated,[111−115] we undertook an AOC calculation on the hypothetical complex $[(TIMEN^{Me})Mn(N)]^{2+}$ with the fluoride ligand removed but with the experimentally determined geometry of **6**. The coordinate system was again chosen with the void in the xz-plane. For this system, the AOC DFT calculation places d(yz) lower (970 cm^{-1}, Figure S20, Supporting Information) in energy than d(xz), which, in the AOM parametrization, forces the e_π^C to be negative (since $e_\sigma^C > 0$) and therefore computes the NHC ligands to be π-acceptors.

The third absorption band of higher intensity, centered at $\lambda \approx 340$ nm, coincides with the AOC-computed position (30 700−33 900 cm^{-1}) of a strongly admixed orbital with significant Mn($3d(z^2)/4p(z)$) character. This assignment hails support from the correlation of this band's intensity with the asymmetry of the LF along the z-axis and the concomitant p–d mixing.

CONCLUSIONS

In summary the concept of coordination-induced spin-state change is not limited to nickel(II) complexes. This was shown by presenting the first example of a high-valent, d^2 manganese complex exhibiting a coordination-induced spin-state change. Starting from the C_3-symmetric, paramagnetic manganese(V) nitrido complex **1** (d^2 high spin, $S = 1$), a series of diamagnetic (d^2 low spin, $S = 0$) tetragonal nitride complexes of the type $[(TIMEN^{xyl})Mn(N)(L)]^{n+}$ ($[\mathbf{2}-\mathbf{7}]^{n+}$: L = MeCN, ^{t}BuNC, CN^-, NCS^-, F^-, μ-$\{Ag(CN)_2\}^-$, with $n = 1, 2$) have been synthesized, by utilizing the moderate flexibility of the $TIMEN^{xyl}$ ligand framework. The reversibility of the spin-state change can be controlled by the choice of L. For L = MeCN a fully reversible TD-CISSS was observed. Thermodynamic parameters for the TD-CISSS could be obtained by integration of VT ^{1}H NMR spectra. It is noteworthy that the tetragonal nitrido complexes described herein are purely diamagnetic and do not show any TIP, as has been shown for other low-spin manganese(V) nitrido moieties within a cyclam ligand framework.[77] IR studies on complexes **3**−**5**, and **7** showed that the Mn–L bond is predominantly σ in nature, although minor contributions from π-backbonding are observed. Correlation of the solid-state molecular structures of the tetragonal manganese(V) nitrido complexes **2**−**6** together with the coupling patterns in the ^{1}H NMR spectra revealed that the complex structure in solution can be assumed to be almost identical to the solid-state structure. Therefore, these systems are ideal to study the relation between complex geometry and electronic structure in solution.

Electronic absorption spectra and supporting LFT and DFT calculations of the approximately electronically tetragonal nitrido complexes suggest a 1 + 2 + 1 + 1 orbital splitting in contrast to the 2 + 2 + 1 orbital splitting found in the trigonal nitrido complex **1**. In the six-coordinate nitrido complexes the symmetry of the equatorial LF is reduced, resulting in a split set (<1000 cm^{-1}) of {d(xz),d(yz)} orbitals. The change of the d-orbital splitting by altering the complex symmetry is the origin of the coordination-induced spin-state change.

In principle, this concept should be applicable to a wide range of coordination compounds, and it is worthwhile to further investigate this phenomenon. Other than classical thermally induced SCO complexes, these systems work under ambient conditions, opening a wide range of potential applications from sensor technologies to medical diagnostics.[58,62,116,117]

EXPERIMENTAL SECTION

General Considerations. All air- and moisture-sensitive experiments were performed under dry nitrogen atmosphere using standard Schlenk techniques or an MBraun inert-gas glovebox containing an

DOI: 10.1021/acs.inorgchem.5b00112
Inorg. Chem. 2015, 54, 3562−3572

atmosphere of purified dinitrogen. *tert*-Butylisocyanide, 98%, and tetrabutylammonium cyanide, 95%, were purchased from Aldrich and used as received. Silver tetraphenylborate, 98%, silver fluoride, 99+%, and silver cyanide, 99%, were purchased from ACROS and were used without further purification. Sodium thiocyanate, 98%, was purchased from Alfa Aesar and used without further purification. Solvents were purified using a two-column solid-state purification system (Glass-contour System, Irvine, CA) and transferred to the glovebox without exposure to air. NMR solvents were obtained packaged under argon and stored over activated molecular sieves and sodium (where appropriate) prior to use. The complexes $[(TIMEN^{xyl})Mn^{IV}(N)]BPh_4$ and $[(TIMEN^{xyl})Mn(N)](PF_6)_2$ ($TIMEN^{xyl}$ = tris[2-(3-(2,6-xylyl)-imidazol-2-ylidene)ethyl]amine) were prepared following our previously described methods.[82] Magnetism data of crystalline powdered samples (10−20 mg) were recorded with a SQUID magnetometer (Quantum Design) at 10 kOe (2−300 K for **4** and **6**). Samples used for magnetization measurement were recrystallized multiple times and checked for chemical composition and purity by elemental analysis (C, H, and N) and/or ^{1}H NMR spectroscopy. Data reproducibility was also carefully checked on independently synthesized samples. ^{1}H NMR spectra were recorded on JEOL ECX 400 MHz instruments operating at respective frequencies of 400.178 MHz with a probe temperature of 23 °C; if not stated otherwise. ^{13}C NMR spectra were recorded on JEOL ECX 400 MHz instruments operating at respective frequencies of 100.624 MHz with a probe temperature of 23 °C. Chemical shifts were reported relative to the chemical shifts of the residual solvent as a secondary standard and were reported in ppm.[118] ^{19}F NMR data were acquired on a JEOL ECX 400 MHz instrument, and chemical shifts were referenced by the delta NMR software. Electronic absorption spectra were recorded from 180 to 1020 nm (**2**) in acetonitrile with a S600 UV−vis spectrophotometer from Jena Analytik and from 200 to 1500 nm with a Shimadzu (UV-3600) UV−vis−near-IR spectrophotometer in acetonitrile. All IR spectra were recorded on a Shimadzu IRAffinity-1 system in KBr pellets. Elemental analysis results were obtained from the Analytical Laboratories at the Friedrich-Alexander University Erlangen-Nürnberg (FAU) (Erlangen, Germany). Whenever elemental analysis data were fit with fractional solvent, the presence of the solvent was independently confirmed by NMR spectroscopy or X-ray diffraction (XRD).

Observation and Characterization of 2. $[(TIMEN^{xyl})Mn(N)(NCMe)](PF_6)_2$. When a solution of **1** in acetonitrile is cooled to temperatures below −10 °C compound **2** forms quantitatively. Crystals of the corresponding bis(tetraphenylborate) salt of **2**, suitable for XRD studies, were obtained by slow evaporation of a concentrated acetonitrile solution of **1** at room temperature, in the presence of sodium tetraphenylborate.

^{1}H NMR (−20 °C, acetonitrile-d_3), δ: 7.42−7.53 (m, 3 H, Ar−H), 7.23 (br. s., 2 H, Ar−H), 7.06 (m, 7 H, Ar−H), 6.91 (m, 2 H, Ar−H), 6.77 (d, J = 5.6 Hz, 1 H, Ar−H), 4.61 (m, 2 H, CH_2), 4.33 (d, J = 14.6 Hz, 1 H, CH_2), 4.15 (d, J = 13.5 Hz, 1 H, CH_2), 3.80 (t, J = 12.8 Hz, 1 H, CH_2), 3.41−3.59 (m, 2 H), CH_2, 3.19 (d, J = 15.5 Hz, 1 H, CH_2), 3.06 (t, J = 12.4 Hz, 1 H, CH_2), 2.91 (d, J = 12.6 Hz, 1 H, CH_2), 2.78 (d, J = 12.8 Hz, 1 H, CH_2), 2.40 (t, J = 11.5 Hz, 1 H, CH_2), 1.68 (br. s, 3 H, CH_3), 1.61 (br. s, 3 H, CH_3), 1.57 (br. s, 3 H, CH_3), 1.47 (br. s, 3 H, CH_3), 0.88 (br. s, 3 H, CH_3), 0.85 (br. s, 3 H, CH_3); ^{13}C NMR (−20 °C, acetonitrile-d_3), δ: 185.61 (1 C, $C_{carbene}$), 181.14 (1 C, $C_{carbene}$), 179.84 (1 C, $C_{carbene}$), 140.21 (1 C, Ar−C), 139.07 (1 C, Ar−C), 138.76 (1 C, Ar−C), 138.29 (1 C, Ar−C), 137.87 (1 C, Ar−C), 137.45 (1 C, Ar−C), 136.44 (1 C, Ar−C), 135.94 (1 C, Ar−C), 130.59 (1 C, Ar−C), 130.41 (1 C, Ar−C), 130.12 (1 C, Ar−C), 129.96 (1 C, Ar−C), 129.79 (1 C, Ar−C), 129.71 (1 C, Ar−C), 129.25 (1 C, Ar−C), 129.13 (1 C, Ar−C), 128.89 (1 C, Ar−C), 128.81 (1 C, Ar−C), 127.99 (1 C, Ar−C), 127.92 (1 C, Ar−C), 127.42 (1 C, Ar−C), 126.97 (1 C, Ar−C), 126.65 (1 C, Ar−C), 126.24 (1 C, Ar−C), 63.37 (1 C, CH_2), 57.55 (1 C, CH_2), 56.47 (1 C, CH_2), 50.27 (1 C, CH_2), 48.93 (1 C, CH_2), 47.91 (1 C, CH_2), 18.39 (1 C, CH_3), 18.16 (1 C, CH_3), 17.95 (1 C, CH_3), 17.59 (1 C, CH_3), 17.43 (1 C, CH_3), 16.78 (1 C, CH_3).

Synthesis of 3. $[(TIMEN^{xyl})Mn(N)(NC^tBu)](BPh_4)_2$. A solution of $[(TIMEN^{xyl})Mn^{IV}(N)]BPh_4$ (48.8 mg, 48.8 μmol) in tetrahydrofuran (THF, 15 mL) was stirred over $AgBPh_4$ (20.8 mg, 48.8 μmol) for 10 min until the color changed from deep red to brown. The reaction mixture was filtered over Celite to give a bright orange filtrate. Excess ^{t}BuNC was added to the filtrate while stirring, and the solution was concentrated (5 mL). After a few minutes, a bright pink precipitate formed. The solid was filtered off and recrystallized by slow diffusion of ether into a concentrated acetonitrile solution. The crystals were collected, washed with ether, and dried in vacuo to yield the title compound in 61% yield (42.1 mg, 30.0 μmol). Slow diffusion of diethyl ether into a concentrated acetonitrile solution afforded single crystals suitable for XRD studies.

CHN elemental analysis (%) for $C_{92}H_{94}N_9B_2Mn$ (calculated/found). C 78.80/78.35, H 6.76/6.74, N 8.99/8.65. ^{1}H NMR (acetonitrile-d_3), δ: 7.56 (d, J = 1.9 Hz, 1 H, Im-H), 7.42 (d, J = 1.9 Hz, 1 H, Im-H), 7.41 (d, J = 1.9 Hz, 1 H, Im-H), 7.28 (d, J = 1.5 Hz, 1 H, Im-H), 7.25−7.31 (m, 16 H, o−Ar−H-BPh_4^-), 7.22 (dd, J = 7.4, 7.3 Hz, 2 H), 7.17 (d, J = 1.9 Hz, 1 H, Im-H), 7.09−7.14 (m, 1 H), 7.09 (dd, J = 7.6 Hz, 1 H, p−Ar-H), 7.03 (d, J = 1.9 Hz, 1 H, Im-H), 7.02−7.04 (m, 1 H), 6.99 (t, J = 7.5 Hz, 17 H, Ar−H), 6.93 (dd, J = 8.9, 7.6 Hz, 2 H, Ar−H), 6.84 (t, J = 7.3 Hz, 8 H p−Ar−H-BPh_4^-), 6.78 (d, J = 7.6 Hz, 1 H, Ar−H), 4.49−4.63 (m, 2 H, CH_2), 4.16 (ddd, J = 15.3, 2.5, 2.4 Hz, 1 H, CH_2), 4.03 (dd, J = 15.5, 4.7 Hz, 1 H, CH_2), 3.58 (dd, J = 13.1 Hz, 1 H, CH_2), 3.35−3.46 (m, 1 H, CH_2), 3.30 (dd, J = 15.6, 9.7 Hz, 1 H, CH_2), 2.91 (ddd, J = 15.6, 2.1, 2.0 Hz, 1 H, CH_2), 2.74−2.84 (m, 2 H, CH_2), 2.72 (dd, J = 13.9, 4.9 Hz, 1 H, CH_2), 2.32 (dd, J = 13.8, 9.5 Hz, 1 H, CH_2), 1.74 (s, 3 H, CH_3), 1.70 (s, 3 H, CH_3), 1.66 (s, 3 H, CH_3), 1.53 (s, 3 H, CH_3), 1.25 (s, 9 H, ^{t}Bu-CH_3), 0.89 (s, 3 H, CH_3), 0.85 (s, 3 H, CH_3); ^{13}C NMR (acetonitrile-d_3), δ: 185.07 (1 C, $C_{carbene}$), 183.30 (1 C, $C_{carbene}$), 181.04 (1 C, $C_{carbene}$), 164.82 (q, 8 C, $J_{B,C}$ = 148.00 Hz, *ipso*-C-BPh_4^-), 149.33 (1 C, C≡N−^{t}Bu), 140.27 (1 C, Ar−C), 140.13 (1 C, Ar−C), 139.19 (1 C, Ar−C), 138.42 (1 C, Ar−C), 137.74 (1 C, Ar−C), 137.49 (1 C, Ar−C), 137.30 (1 C, Ar−C), 136.83 (1 C, Ar−C), 136.76 (16 C, o-C-BPh_4^-), 136.24 (1 C, Ar−C), 131.08 (1 C, Ar−C), 130.66 (1 C, Ar−C), 130.46 (1 C, Ar−C), 130.43 (1 C, Ar−C), 130.20 (1 C, Ar−C), 129.64 (1 C, Ar−C), 129.46 (1 C, Ar−C), 129.40 (1 C, Ar−C), 129.23 (1 C, Ar−C), 128.95 (1 C, Ar−C), 128.90 (1 C, Ar−C), 128.25 (1 C, Ar−C), 127.90 (1 C, Ar−C), 127.53 (1 C, Ar−C), 126.63 (16 C, m-C-BPh_4^-), 126.07 (1 C, Ar−C), 122.80 (8 C, p-C-BPh_4^-), 63.45 (1 C, CH_2), 62.79 (1 C, ^{t}Bu-C), 59.01 (1 C, CH_2), 56.07 (1 C, CH_2), 50.25 (1 C, CH_2), 48.81(1 C, CH_2), 48.24 (1 C, CH_2), 29.98 (3 C, ^{t}Bu-CH_3), 19.03 (1 C, CH_3), 19.01 (1 C, CH_3), 18.42 (1 C, CH_3), 18.32 (1 C, CH_3), 17.94 (1 C, CH_3), 16.97 (1 C, CH_3). IR: (ν_{CN}− = 2185 cm^{-1}).

Synthesis of 4. $[(TIMEN^{xyl})Mn(N)(CN)]BPh_4$. A solution of $[(TIMEN^{xyl})Mn^{IV}(N)]BPh_4$ (24.0 mg, 24.0 μmol) in THF (15 mL) was stirred over $AgBPh_4$ (10.3 mg, 24.0 μmol) for 10 min until the color changed from deep red to brown. The reaction mixture was filtered over Celite to give a bright orange filtrate. After addition of excess tetrabutylammonium cyanide to the filtrate the color changed to light pink. The solvent was removed in vacuo to give a light pink solid. 1,2-Dimethoxyethane (DME, 15 mL) was added, and the resulting suspension was stirred overnight and then filtered over Celite; the remaining solid was washed with DME (2 mL) and washed from the Celite plug with acetonitrile (5 mL). The resulting solution was concentrated close to dryness and dissolved in THF (0.5 mL). Slow diffusion of ether into this solution yielded the crystalline title compound in 40% yield (9.8 mg, 9.6 μmol). Single crystals suitable for XRD studies could be obtained by the same procedure or by slow evaporation of a concentrated DME solution of **4**.

CHN elemental analysis (%) for $C_{64}H_{65}N_9BMn·1.4$ THF (calculated/found). C 74.18/73.71, H 6.82/6.55, N 11.19/11.62. ^{1}H NMR (acetonitrile-d_3), δ: 7.41 (d, J = 1.9 Hz, 1 H, Im-H), 7.34 (d, J = 1.9 Hz, 1 H, Im-H), 7.29 (d, J = 2.2 Hz, 1 H, Im-H), 7.28 (d, J = 1.4 Hz, 1 H, Im-H), 7.25−7.31 (m, 8 H, o−Ar−H-BPh_4^-), 7.13 (d, J = 7.6 Hz, 1 H, Ar−H), 7.12 (dd, J = 7.6 Hz, 1 H, Ar−H), 7.08 (dd, J = 7.5 Hz, 1 H, Ar−H), 7.05 (d, J = 7.6 Hz, 1 H, Ar−H), 6.99 (t, J = 7.5 Hz, 8 H, m−Ar−H-BPh_4^-), 6.96 (d, J = 1.9 Hz, 1 H, Im-H), 6.90 (d, J = 1.9 Hz, 1 H, Im-H), 6.87−6.94 (m, 3 H, Ar−H), 6.84 (tt, J = 7.2, 1.5 Hz, 4 H, p−Ar−H-BPh_4^-), 6.76 (dd, J = 12.7, 7.6 Hz, 2 H, Ar−H), 4.37−4.59

DOI: 10.1021/acs.inorgchem.5b00112
Inorg. Chem. 2015, 54, 3562−3572

(m, 3 H, CH_2), 4.09 (ddd, J = 14.9, 2.4, 2.3 Hz, 1 H, CH_2), 3.93 (dd, J = 15.1, 4.8 Hz, 1 H, CH_2), 3.74 (ddd, J = 13.7, 13.5, 1.6 Hz, 1 H, CH_2), 3.19 (dd, J = 15.1, 9.5 Hz, 1 H, CH_2), 2.85 (d, J = 15.4 Hz, 1 H, CH_2), 2.60−2.66 (m, 1 H, CH_2), 2.60 (dd, J = 13.5, 5.0 Hz, 1 H, CH_2), 2.48 (m, J = 11.9, 5.0, 1.0 Hz, 1 H, CH_2), 2.29 (dd, J = 13.6, 9.4 Hz, 1 H, CH_2), 1.83 (s, 3 H, CH_3), 1.68 (s, 6 H, CH_3), 1.56 (s, 3 H, CH_3), 1.08 (s, 3 H, CH_3), 0.76 (s, 3 H, CH_3); ^{13}C NMR (acetonitrile-d_3), δ: 193.28 (1 C, $C_{carbene}$), 190.10 (1 C, $C_{carbene}$), 188.31 (1 C, $C_{carbene}$), 164.82 (q, 4 C, $J_{B,C}$ = 148.00 Hz, *ipso*-C-BPh_4^-), 148.01 (1 C, Ar−C), 141.18 (1 C, Ar−C), 140.39 (1 C, Ar−C), 140.10 (1 C, Ar−C), 139.76 (1 C, Ar−C), 139.19 (1 C, Ar−C), 138.79 (1 C, Ar−C), 136.98 (1 C, Ar−C), 136.74 (8 C, *o*-C-BPh_4^-), 136.32 (1 C, Ar−C), 136.11 (1 C, Ar−C), 130.23 (1 C, Ar−C), 129.84 (1 C, Ar−C), 129.54 (1 C, Ar−C), 129.22 (1 C, Ar−C), 129.02 (1 C, Ar−C), 128.95 (1 C, Ar−C), 128.84 (1 C, Ar−C), 127.62 (1 C, Ar−C), 127.32 (1 C, Ar−C), 127.25 (1 C, Ar−C), 126.86 (1 C, Ar−C), 126.59 (8 C, *m*-C-BPh_4^-), 126.45 (1 C, Ar−C), 125.33 (1 C, Ar−C), 125.08 (1 C, Ar−C), 122.78 (4 C, *p*-C-BPh_4^-), 115.70 (1 C, Ar−C), 62.75 (1 C, CH_2), 57.99 (1 C, CH_2), 56.30 (1 C, CH_2), 50.13 (1 C, CH_2), 48.98 (1 C, CH_2), 48.54 (1 C, CH_2), 20.44 (1 C, CH_3), 19.17 (1 C, CH_3), 18.62 (1 C, CH_3), 17.98 (1 C, CH_3), 17.49 (1 C, CH_3), 17.17 (1 C, CH_3). IR: (ν_{CN^-} = 2120 cm^{-1}).

Synthesis of 5. [(TIMEN^{xyl})Mn(N)(SCN)]BPh_4. A solution of [(TIMEN^{xyl})Mn^{IV}(N)]BPh_4 (33.7 mg, 33.7 μmol) in THF (15 mL) was stirred over $AgBPh_4$ (14.4 mg, 33.7 μmol) for 10 min until the color changed from deep red to brown. The reaction mixture was filtered over Celite to give a bright orange filtrate. After addition of excess NaSCN the filtrate turned purple. The solvent was removed, and the resulting solid was extracted with CH_2Cl_2 and filtered over Celite. The solvent was removed in vacuo to give a purple solid. The solid was extracted into acetonitrile (1.5 mL), and slow diffusion of ether into this solution yielded the crystalline title compound in 58% yield (20.5 mg, 19.4 μmol). Single crystals suitable for XRD studies could be obtained by the same procedure.

CHNS elemental analysis (%) for $C_{64}H_{65}N_9BMnS{\cdot}0.9Et_2O$ (calculated/found). C 72.18/72.37, H 6.63/6.64, N 11.21/11.04, S 2.85/2.74. ^{1}H NMR (acetonitrile-d_3), δ: 7.44 (d, J = 1.9 Hz, 1 H, Im-H), 7.40 (d, J = 1.9 Hz, 1 H, Im-H), 7.28 (d, J = 1.9 Hz, 1 H, Im-H), 7.27 (d, J = 1.4 Hz, 1 H, Im-H), 7.24−7.30 (m, 8 H, *o*-Ar−H-BPh_4^-), 7.17 (dd, J = 7.7, 7.6 Hz, 1 H, *p*-Ar-H), 7.12 (dd, J = 7.7, 7.6 Hz, 1 H, *p*-Ar-H), 7.06 (dd, J = 7.7, 7.6 Hz, 1 H, *p*-Ar-H), 6.99 (t, J = 7.6 Hz, 8 H, *m*-Ar−H-BPh_4^-), 6.93−7.04 (m, 4 H, Ar−H), 6.92 (d, J = 1.9 Hz, 1 H, Im-H), 6.89 (d, J = 6.2 Hz, 1 H, Ar−H), 6.87 (d, J = 1.9 Hz, 1 H, Im-H), 6.84 (tt, J = 7.2, 1.5 Hz, 4 H, *p*-Ar−H-BPh_4^-), 6.77 (d, J = 7.6 Hz, 1 H, Ar−H), 4.45−4.62 (m, 2 H, CH_2), 4.22 (ddd, J = 14.8, 2.2 Hz, 1 H, CH_2), 4.02 (dd, J = 15.0, 4.7 Hz, 1 H, CH_2), 3.85 (m, J = 13.0, 13.0 Hz, 2 H, CH_2), 3.33−3.41 (m, 1 H, CH_2), 3.13 (d, J = 15.5 Hz, 1 H, CH_2), 2.87−2.97 (m, 1 H, CH_2), 2.81 (dd, J = 13.6, 4.9 Hz, 1 H, CH_2), 2.71 (ddd, J = 12.8, 3.6, 2.2 Hz, 1 H, CH_2), 2.35 (dd, J = 13.7, 9.5 Hz, 1 H, CH_2), 1.70 (s, 6 H, CH_3), 1.63 (s, 3 H, CH_3), 1.51 (s, 3 H, CH_3), 0.95 (s, 3 H, CH_3), 0.88 (s, 3 H, CH_3); ^{13}C NMR (acetonitrile-d_3), δ: 192.08 (1 C, $C_{carbene}$), 186.02 (1 C, $C_{carbene}$), 185.32 (1 C, $C_{carbene}$), 164.80 (q, 8 C, $J_{B,C}$ = 148.00 Hz, *ipso*-C-BPh_4^-), 141.05 (1 C, Ar−C), 139.68 (1 C, Ar−C), 139.63 (1 C, Ar−C), 139.01 (1 C, Ar−C), 138.83 (1 C, Ar−C), 138.76(1 C, Ar−C), 136.74 (8 C, *o*-C-BPh_4^-), 136.34 (1 C, Ar−C), 136.06 (1 C, Ar−C), 130.34 (1 C, Ar−C), 130.16 (1 C, Ar−C), 129.85 (1 C, Ar−C), 129.59 (1 C, Ar−C), 129.32 (1 C, Ar−C), 129.20(1 C, Ar−C), 129.09 (1 C, Ar−C), 128.47 (1 C, Ar−C), 128.07 (1 C, Ar−C), 128.01 (1 C, Ar−C), 127.73 (1 C, Ar−C), 126.83 (1 C, Ar−C), 126.58 (8 C, *m*-C-BPh_4^-), 125.72 (1 C, Ar−C), 125.61 (1 C, Ar−C), 125.16 (1 C, Ar−C), 122.77 (4 C, *p*-C-BPh_4^-), 115.73 (1 C, Ar−C), 63.31 (1 C, CH_2), 57.43 (1 C, CH_2), 56.80 (1 C, CH_2), 50.49 (1 C, CH_2), 49.32 (1 C, CH_2), 48.72 (1 C, CH_2), 18.83 (1 C, CH_3), 18.53 (1 C, CH_3), 18.18 (1 C, CH_3), 17.90 (1 C, CH_3), 17.43 (1 C, CH_3), 17.10 (1 C, CH_3). IR: (ν_{CN^-} = 2085 cm^{-1}).

Synthesis of 6. [(TIMEN^{xyl})Mn(N)(F)]BPh_4. A solution of [(TIMEN^{xyl})Mn^{IV}(N)]BPh_4 (32.0 mg, 32.0 μmol) in CH_2Cl_2 (3 mL) was stirred with AgF (4.1 mg, 32.0 μmol) overnight. The resulting solution was filtered over Celite, and the solvent was removed in vacuo. The resulting solid was dissolved in the minimum amount of THF. Slow diffusion of ether into this THF solution yielded the crystalline title compound in 75% yield (24.6 mg, 24.1 μmol). Single crystals suitable for XRD studies could be obtained by the same procedure.

CHN elemental analysis (%) for $C_{63}H_{65}N_8BFMn{\cdot}0.77$ THF (calculated/found). C 73.86/73.34, H 6.68/6.15, N 10.43/9.96. ^{1}H NMR (acetonitrile-d_3), δ: 7.35 (d, J = 1.9 Hz, 1 H, Im-H), 7.28 (d, J = 1.4 Hz, 1 H, Im-H), 7.24−7.30 (m, 8 H, *o*-Ar−H-BPh_4^-), 7.15 (d, J = 1.9 Hz, 1 H, Im-H), 7.14 (dd, J = 7.5 Hz, 1 H, *p*-Ar-H), 7.11 (dd, J = 7.6 Hz, 1 H, *p*-Ar-H), 7.05 (dd, J = 7.6 Hz, 1 H, *p*-Ar-H), 6.84 (tt, J = 7.2, 1.5 Hz, 4 H, *p*-Ar−H-BPh_4^-), 6.80 (d, J = 1.9 Hz, 1 H, Im-H), 6.78 (d, J = 1.9 Hz, 1 H, Im-H), 6.76 (d, J = 7.6 Hz, 2 H, Ar−H), 4.43−4.53 (m, 1 H, CH_2), 4.38 (ddd, J = 15.3, 3.5, 2.9 Hz, 1 H, CH_2), 4.17 (ddd, J = 14.5, 2.3 Hz, 1 H, CH_2), 4.07−4.24 (m, 1 H, CH_2), 3.95 (dd, J = 14.8, 4.7 Hz, 1 H, CH_2), 3.88 (ddd, J = 14.5, 12.8, 1.5 Hz, 1 H, CH_2), 3.34 (dd, J = 14.8, 9.5 Hz, 1 H, CH_2), 3.19 (d, J = 15.2 Hz, 1 H, CH_2), 2.89 (t, J = 13.5 Hz, 1 H, CH_2), 2.80 (dd, J = 13.5, 4.8 Hz, 1 H, CH_2), 2.49 (d, J = 11.3 Hz, 1 H, CH_2), 2.31 (dd, J = 13.6, 9.4 Hz, 1 H, CH_2), 1.78 (s, 3 H, CH_3), 1.64 (s, 3 H, CH_3), 1.55 (s, 3 H, CH_3), 1.44 (s, 3 H, CH_3), 1.06 (s, 3 H, CH_3), 0.92 (s, 3 H, CH_3); ^{13}C NMR (acetonitrile-d_3), δ: 196.49 (1 C, $C_{carbene}$), 190.85 (1 C, $C_{carbene}$), 189.63 (1 C, $C_{carbene}$), 164.83 (q, 8 C, $J_{B,C}$ = 148.00 Hz, *ipso*-C-BPh_4^-), 141.61 (1 C, Ar−C), 140.42 (1 C, Ar−C), 140.12 (1 C, Ar−C), 139.99 (1 C, Ar−C), 139.42 (1 C, Ar−C), 139.05 (1 C, Ar−C), 137.04 (1 C, Ar−C), 136.75 (8 C, *o*-C-BPh_4^-), 135.96 (1 C, Ar−C), 135.84 (1 C, Ar−C), 130.05 (1 C, Ar−C), 129.66 (1 C, Ar−C), 129.36 (1 C, Ar−C), 129.30 (1 C, Ar−C), 129.17 (1 C, Ar−C), 129.13 (1 C, Ar−C), 128.90 (1 C, Ar−C), 127.79 (1 C, Ar−C), 127.48 (1 C, Ar−C), 127.11 (1 C, Ar−C), 126.89 (1 C, Ar−C), 126.60 (8 C, *m*-C-BPh_4^-), 125.31 (2 C, Ar−C), 124.10 (1 C, Ar−C), 123.53 (1 C, Ar−C), 122.78 (4 C, *p*-C-BPh_4^-), 63.19 (1 C, CH_2), 56.71 (1 C, CH_2), 56.54 (1 C, CH_2), 50.71 (1 C, CH_2), 49.65 (1 C, CH_2), 49.05 (1 C, CH_2), 19.00 (1 C, CH_3), 18.62 (1 C, CH_3), 17.84 (1 C, CH_3), 17.64 (1 C, CH_3), 17.29 (1 C, CH_3), 17.18 (1 C, CH_3); ^{19}F NMR (377 MHz, 23 °C, acetonitrile-d_3), δ: −324.87 (s).

Synthesis of 7. [{(TIMEN^{xyl})Mn(N)}$_2$μ-{Ag(CN_2)}]$(BPh_4)_3$. A solution of [(TIMEN^{xyl})Mn^{IV}(N)]BPh_4 (70.0 mg, 70.0 μmol) in acetonitrile (3 mL) was stirred over AgCN (11.4 mg, 85.1 μmol) for 3 d and filtered over Celite to give a pink solution. The resulting solution was concentrated, and slow diffusion of diethyl ether or benzene into this solution reproducibly yielded very few single crystals of the title compound suitable for XRD studies. Despite multiple attempts, the pure compound could not be obtained in bulk quantities for full characterization. The IR spectrum of the solid only showed one single stretch in the region from 2050−2250 cm^{-1}, which we assign to the CN^- stretching frequency in 7. IR: (ν_{CN^-} = 2185 cm^{-1}).

■ ASSOCIATED CONTENT

Ⓢ Supporting Information

Crystallographic details, NMR spectra, Gaussian deconvolution of electronic absorption spectra, LF calculations, DFT calculations, crystallographic data in CIF file, references. This material is available free of charge via the Internet at http://pubs.acs.org.

■ AUTHOR INFORMATION

Corresponding Author

*E-mail: Karsten.Meyer@fau.de. Phone: +49 (0)9131 8527361. Fax: +49(0)9131 8527367.

Notes

The authors declare no competing financial interest.

■ ACKNOWLEDGMENTS

We thank the Friedrich-Alexander University Erlangen-Nürnberg (FAU) for generous financial support. Support of this work by COST Action CM1305 ECOSTBio (Explicit

DOI: 10.1021/acs.inorgchem.5b00112
Inorg. Chem. 2015, 54, 3562−3572

Control Over Spin-States in Technology and Biochemistry) is acknowledged. J.B. acknowledges support from the Danish Research Council for Independent Research (Grant No. 12-125226).

REFERENCES

(1) *Spin-Crossover Materials: Properties and Applications;* Halcrow, M. A., ed.; Wiley: Hoboken, NJ, 2013.
(2) *Spin Crossover in Transition Metal Compounds I–III;* Springer-Verlag: Berlin, Germany, 2004; Vol. *233–235*.
(3) Boillot, M.-L.; Zarembowitch, J.; Sour, A. *Top. Curr. Chem.* **2004**, *234*, 261–276.
(4) Weber, B. *Coord. Chem. Rev.* **2009**, *253*, 2432–2449.
(5) Šalitroš, I.; Madhu, N. T.; Boča, R.; Pavlik, J.; Ruben, M. *Monatsh. Chem.* **2009**, *140*, 695–733.
(6) Grohmann, A.; Haryono, M.; Student, K.; Müller, P.; Stocker, M. *Eur. J. Inorg. Chem.* **2013**, 662–669.
(7) Special Issue: Spin-Crossover Complexes (Cluster Issue); Murray, K. S.; Oshio, H., Real, J. A. *Eur. J. Inorg. Chem.*, **2013**.
(8) Bousseksou, A.; Molnár, G.; Salmon, L.; Nicolazzi, W. *Chem. Soc. Rev.* **2011**, *40*, 3313–3335.
(9) Gütlich, P. *Eur. J. Inorg. Chem.* **2013**, 581–591.
(10) Gütlich, P.; Gaspar, A. B.; Garcia, Y. *Beilstein J. Org. Chem.* **2013**, *9*, 342–391.
(11) Bousseksou, A.; Molnár, G.; Real, J. A.; Tanaka, K. *Coord. Chem. Rev.* **2007**, *251*, 1822–1833.
(12) Olguin, J.; Brooker, S. *Coord. Chem. Rev.* **2011**, *255*, 203–240.
(13) Real, J. A.; Andres, E.; Munoz, M. C.; Julve, M.; Granier, T.; Bousseksou, A.; Varret, F. *Science* **1995**, *268*, 265–267.
(14) Bonhommeau, S.; Molnár, G.; Galet, A.; Zwick, A.; Real, J.-A.; McGarvey, J. J.; Bousseksou, A. *Angew. Chem., Int. Ed.* **2005**, *44*, 4069–4073.
(15) Bonnet, S.; Siegler, M. A.; Costa, J. S.; Molnár, G.; Bousseksou, A.; Spek, A. L.; Gamez, P.; Reedijk, J. *Chem. Commun.* **2008**, 5619–5621.
(16) Cobo, S.; Ostrovskii, D.; Bonhommeau, S.; Vendier, L.; Molnár, G.; Salmon, L.; Tanaka, K.; Bousseksou, A. *J. Am. Chem. Soc.* **2008**, *130*, 9019–9024.
(17) Fedaoui, D.; Bouhadja, Y.; Kaiba, A.; Guionneau, P.; Létard, J.-F.; Rosa, P. *Eur. J. Inorg. Chem.* **2008**, 1022–1026.
(18) Mishra, V.; Mukherjee, R.; Linares, J.; Balde, C.; Desplanches, C.; Létard, J.-F.; Collet, E.; Toupet, L.; Castro, M.; Varret, F. *Inorg. Chem.* **2008**, *47*, 7577–7587.
(19) Neville, S. M.; Halder, G. J.; Chapman, K. W.; Duriska, M. B.; Southon, P. D.; Cashion, J. D.; Létard, J.-F.; Moubaraki, B.; Murray, K. S.; Kepert, C. J. *J. Am. Chem. Soc.* **2008**, *130*, 2869–2876.
(20) Weber, B.; Carbonera, C.; Desplances, C.; Létard, J.-F. *Eur. J. Inorg. Chem.* **2008**, 1589–1598.
(21) Weber, B.; Kaps, E.; Weigand, J.; Carbonera, C.; Létard, J.-F.; Achterhold, K.; Parak, F. G. *Inorg. Chem.* **2008**, *47*, 487–496.
(22) Weber, B.; Kaps, E. S.; Desplanches, C.; Létard, J.-F. *Eur. J. Inorg. Chem.* **2008**, 2963–2966.
(23) Weber, B.; Kaps, E. S.; Desplanches, C.; Létard, J.-F.; Achterhold, K.; Parak, F. G. *Eur. J. Inorg. Chem.* **2008**, 4891–4898.
(24) Létard, J.-F.; Carbonera, C.; Real, J. A.; Kawata, S.; Kaizaki, S. *Chem.—Eur. J.* **2009**, *15*, 4146–4155.
(25) Mishra, V.; Mishra, H.; Mukherjee, R.; Codjovi, E.; Linares, J.; Létard, J.-F.; Desplanches, C.; Balde, C.; Enachescu, C.; Varret, F. *Dalton Trans.* **2009**, 7462–7472.
(26) Pritchard, R.; Lazar, H.; Barrett, S. A.; Kilner, C. A.; Asthana, S.; Carbonera, C.; Létard, J.-F.; Halcrow, M. A. *Dalton Trans.* **2009**, 6656–6666.
(27) Amoore, J. J. M.; Neville, S. M.; Moubaraki, B.; Iremonger, S. S.; Murray, K. S.; Létard, J.-F.; Kepert, C. J. *Chem.—Eur. J.* **2010**, *16*, 1973–1982.
(28) Scepaniak, J. J.; Harris, T. D.; Vogel, C. S.; Sutter, J.; Meyer, K.; Smith, J. M. *J. Am. Chem. Soc.* **2011**, *133*, 3824–3827.
(29) Ross, T. M.; Moubaraki, B.; Turner, D. R.; Halder, G. J.; Chastanet, G.; Neville, S. M.; Cashion, J. D.; Létard, J.-F.; Batten, S. R.; Murray, K. S. *Eur. J. Inorg. Chem.* **2011**, 1395–1417.
(30) Mondal, A.; Li, Y.; Herson, P.; Seuleiman, M.; Boillot, M.-L.; Riviere, E.; Julve, M.; Rechignat, L.; Bousseksou, A.; Lescouezec, R. *Chem. Commun.* **2012**, *48*, 5653–5655.
(31) Shepherd, H. J.; Palamarciuc, T.; Rosa, P.; Guionneau, P.; Molnár, G.; Létard, J.-F.; Bousseksou, A. *Angew. Chem., Int. Ed.* **2012**, *51*, 3910–3914.
(32) Létard, J.-F.; Asthana, S.; Shepherd, H. J.; Guionneau, P.; Goeta, A. E.; Suemura, N.; Ishikawa, R.; Kaizaki, S. *Chem.—Eur. J.* **2012**, *18*, 5924–5934.
(33) Shepherd, H. J.; Gural'skiy, I. A.; Quintero, C. M.; Tricard, S.; Salmon, L.; Molnár, G.; Bousseksou, A. *Nat. Commun.* **2013**, *4*, 2607.
(34) Peng, H.; Tricard, S.; Felix, G.; Molnár, G.; Nicolazzi, W.; Salmon, L.; Bousseksou, A. *Angew. Chem., Int. Ed.* **2014**, *53*, 10894–10898.
(35) Mondal, A.; Li, Y.; Chamoreau, L.-M.; Seuleiman, M.; Rechignat, L.; Bousseksou, A.; Boillot, M.-L.; Lescouezec, R. *Chem. Commun.* **2014**, *50*, 2893–2895.
(36) Krüger, H.-J. *Coord. Chem. Rev.* **2009**, *253*, 2450–2459.
(37) Boca, R.; Nemec, I.; Salitros, I.; Pavlik, J.; Herchel, R.; Renz, F. *Pure Appl. Chem.* **2009**, *81*, 1357–1383.
(38) Hayami, S.; Hiki, K.; Kawahara, T.; Maeda, Y.; Urakami, D.; Inoue, K.; Ohama, M.; Kawata, S.; Sato, O. *Chem.—Eur. J.* **2009**, *15*, 3497–3508.
(39) Imatomi, S.; Hashimoto, S.; Matsumoto, N. *Eur. J. Inorg. Chem.* **2009**, 721–726.
(40) Weber, B.; Jäger, E.-G. *Eur. J. Inorg. Chem.* **2009**, 465–477.
(41) Tang, J.; Sanchez Costa, J.; Smulders, S.; Molnár, G.; Bousseksou, A.; Teat, S. J.; Li, Y.; van Albada, G. A.; Gamez, P.; Reedijk, J. *Inorg. Chem.* **2009**, *48*, 2128–2135.
(42) Clemente-Leon, M.; Coronado, E.; Lopez-Jorda, M.; Waerenborgh, J. C. *Inorg. Chem.* **2011**, *50*, 9122–9130.
(43) Bowman, A. C.; Milsmann, C.; Bill, E.; Turner, Z. R.; Lobkovsky, E.; DeBeer, S.; Wieghardt, K.; Chirik, P. J. *J. Am. Chem. Soc.* **2011**, *133*, 17353–17369.
(44) Clemente-Leon, M.; Coronado, E.; Lopez-Jorda, M.; Desplanches, C.; Asthana, S.; Wang, H.; Létard, J.-F. *Chem. Sci.* **2011**, *2*, 1121–1127.
(45) Griffin, M.; Shakespeare, S.; Shepherd, H. J.; Harding, C. J.; Létard, J.-F.; Desplanches, C.; Goeta, A. E.; Howard, J. A. K.; Powell, A. K.; Mereacre, V.; Garcia, Y.; Naik Anil, D.; Müller-Bunz, H.; Morgan, G. G. *Angew. Chem., Int. Ed.* **2011**, *50*, 896–900.
(46) Hayami, S.; Komatsu, Y.; Shimizu, T.; Kamihata, H.; Lee, Y. H. *Coord. Chem. Rev.* **2011**, *255*, 1981–1990.
(47) Carbonera, C.; Dei, A.; Létard, J.-F.; Sangregorio, C.; Sorace, L. *Angew. Chem., Int. Ed.* **2004**, *43*, 3136–3138.
(48) Le Bris, R.; Tsunobuchi, Y.; Mathoniere, C.; Tokoro, H.; Ohkoshi, S.-i.; Ould-Moussa, N.; Molnár, G.; Bousseksou, A.; Létard, J.-F. *Inorg. Chem.* **2012**, *51*, 2852–2859.
(49) Garcia, Y.; Gütlich, P. *Top. Curr. Chem.* **2004**, *234*, 49–62.
(50) Kläui, W. *Z. Naturforsch.* **1979**, *34B*, 1403–1407.
(51) Kläui, W. J. *Chem. Soc., Chem. Commun.* **1979**, 700.
(52) Kläui, W.; Eberspach, W.; Gütlich, P. *Inorg. Chem.* **1987**, *26*, 3977–3982.
(53) Witt, A.; Heinemann, F. W.; Sproules, S.; Khusniyarov, M. M. *Chem.—Eur. J.* **2014**, *20*, 11149–11162.
(54) Kudryavtsev, A. B.; Frauendienst, G.; Linert, W. *J. Coord. Chem.* **1998**, *46*, 221–232.
(55) Ohtsu, H.; Tanaka, K. *Inorg. Chem.* **2004**, *43*, 3024–3030.
(56) Achey, D.; Meyer, G. J. *Inorg. Chem.* **2013**, *52*, 9574–9582.
(57) Thies, S.; Bornholdt, C.; Köhler, F.; Sönnichsen, F. D.; Näther, C.; Tuczek, F.; Herges, R. *Chem.—Eur. J.* **2010**, *16*, 10074–10083.
(58) Thies, S.; Sell, H.; Schütt, C.; Bornholdt, C.; Näther, C.; Tuczek, F.; Herges, R. *J. Am. Chem. Soc.* **2011**, *133*, 16243–16250.
(59) Venkataramani, S.; Jana, U.; Dommaschk, M.; Sönnichsen, F. D.; Tuczek, F.; Herges, R. *Science* **2011**, *331*, 445–448.

DOI: 10.1021/acs.inorgchem.5b00112
Inorg. Chem. 2015, 54, 3562–3572

(60) Thies, S.; Sell, H.; Bornholdt, C.; Schütt, C.; Köhler, F.; Tuczek, F.; Herges, R. *Chem.—Eur. J.* **2012**, *18*, 16358−16368.
(61) Dommaschk, M.; Schütt, C.; Venkataramani, S.; Jana, U.; Näther, C.; Sönnichsen, F. D.; Herges, R. *Dalton Trans.* **2014**, *43*, 17395−17405.
(62) Dommaschk, M.; Gutzeit, F.; Boretius, S.; Haag, R.; Herges, R. *Chem. Commun.* **2014**, *50*, 12476−12478.
(63) Birk, T.; Bendix, J. *Inorg. Chem.* **2003**, *42*, 7608−7615.
(64) Betley, T. A.; Peters, J. C. *J. Am. Chem. Soc.* **2004**, *126*, 6252−6254.
(65) Vogel, C.; Heinemann, F. W.; Sutter, J.; Anthon, C.; Meyer, K. *Angew. Chem., Int. Ed.* **2008**, *47*, 2681−2684.
(66) Saouma, C. T.; Peters, J. C. *Coord. Chem. Rev.* **2011**, *255*, 920−937.
(67) Scepaniak, J. J.; Vogel, C. S.; Khusniyarov, M. M.; Heinemann, F. W.; Meyer, K.; Smith, J. M. *Science* **2011**, *331*, 1049−1052.
(68) Griffith, W. P. *Coord. Chem. Rev.* **1972**, *8*, 369−396.
(69) Dehnicke, K.; Strähle, J. *Angew. Chem., Int. Ed. Engl.* **1992**, *31*, 955−978.
(70) Eikey, R. A.; Abu-Omar, M. M. *Coord. Chem. Rev.* **2003**, *243*, 83−124.
(71) Hill, C. L.; Hollander, F. J. *J. Am. Chem. Soc.* **1982**, *104*, 7318−7319.
(72) Buchler, J. W.; Dreher, C.; Lay, K. L.; Lee, Y. J.; Scheidt, W. R. *Inorg. Chem.* **1983**, *22*, 888−891.
(73) Du Bois, J.; Hong, J.; Carreira, E. M.; Day, M. W. *J. Am. Chem. Soc.* **1996**, *118*, 915−916.
(74) Niemann, A.; Bossek, U.; Haselhorst, G.; Wieghardt, K.; Nuber, B. *Inorg. Chem.* **1996**, *35*, 906−915.
(75) Du Bois, J.; Tomooka, C. S.; Hong, J.; Carreira, E. M.; Day, M. W. *Angew. Chem., Int. Ed. Engl.* **1997**, *36*, 1645−1647.
(76) Chang, C. J.; Connick, W. B.; Low, D. W.; Day, M. W.; Gray, H. B. *Inorg. Chem.* **1998**, *37*, 3107−3110.
(77) Meyer, K.; Bendix, J.; Metzler-Nolte, N.; Weyhermüller, T.; Wieghardt, K. *J. Am. Chem. Soc.* **1998**, *120*, 7260−7270.
(78) Jepsen, A. S.; Roberson, M.; Hazell, R. G. *Chem. Commun.* **1998**, 1599−1600.
(79) Grapperhaus, C. A.; Bill, E.; Weyhermüller, T.; Neese, F.; Wieghardt, K. *Inorg. Chem.* **2001**, *40*, 4191−4198.
(80) Berry, J. F.; Bill, E.; Bothe, E.; DeBeer George, S.; Mienert, B.; Neese, F.; Wieghardt, K. *Science* **2006**, *312*, 1937−1941.
(81) Izzet, G.; Ishow, E.; Delaire, J.; Afonso, C.; Tabet, J. C.; Proust, A. *Inorg. Chem.* **2009**, *48*, 11865−11870.
(82) Kropp, H.; King, A. E.; Khusniyarov, M. M.; Heinemann, F. W.; Lancaster, K. M.; DeBeer, S.; Bill, E.; Meyer, K. *J. Am. Chem. Soc.* **2012**, *134*, 15538−15544.
(83) Hu, X.; Castro-Rodriguez, I.; Meyer, K. *J. Am. Chem. Soc.* **2004**, *126*, 13464−13473.
(84) Bendix, J.; Meyer, K.; Weyhermüller, T.; Bill, E.; Metzler-Nolte, N.; Wieghardt, K. *Inorg. Chem.* **1998**, *37*, 1767−1775.
(85) Karplus, M. *J. Am. Chem. Soc.* **1963**, *85*, 2870−2871.
(86) Hesse, M.; Meier, H., Zeeh, B. *Spektroskopische Methoden in der organischen Chemie;* Thieme: Stuttgart, Germany, 2002.
(87) Scheurer, A.; Maid, H.; Hampel, F.; Saalfrank, R. W.; Toupet, L.; Mosset, P.; Puchta, R.; van Eikema Hommes, N. J. R. *Eur. J. Org. Chem.* **2005**, 2566−2574.
(88) National Institute of Advanced Industrial Science and Technology: http://sdbs.db.aist.go.jp (accessed March 24, 2015).
(89) Chadwick, B. M.; Frankiss, S. G. *J. Mol. Struct.* **1968**, *2*, 281−285.
(90) Strandberg, M. W. P.; Pearsall, C. S.; Weiss, M. T. *J. Chem. Phys.* **1949**, *17*, 429−430.
(91) Davies, P. B.; Hamilton, P. A.; Rothwell, W. J. *J. Chem. Phys.* **1984**, *81*, 1598−1599.
(92) Foster, S. C.; McKellar, A. R. W.; Sears, T. J. *J. Chem. Phys.* **1984**, *81*, 578−579.
(93) Sanchez, R.; Arrington, C.; Arrington, C. A., Jr. *J. Am. Chem. Soc.* **1989**, *111*, 9110−9111.
(94) Selg, P.; Brintzinger, H. H.; Andersen, R. A.; Horvath, I. T. *Angew. Chem., Int. Ed. Engl.* **1995**, *34*, 791−793.
(95) Bodenbinder, M.; Balzer-Joellenbeck, G.; Willner, H.; Batchelor, R. J.; Einstein, F. W. B.; Wang, C.; Aubke, F. *Inorg. Chem.* **1996**, *35*, 82−92.
(96) Selg, P.; Brintzinger, H. H.; Schultz, M.; Andersen, R. A. *Organometallics* **2002**, *21*, 3100−3107.
(97) Haakansson, M.; Jagner, S. *Inorg. Chem.* **1990**, *29*, 5241−5244.
(98) Willner, H.; Aubke, F. *Inorg. Chem.* **1990**, *29*, 2195−2200.
(99) Hurlburt, P. K.; Anderson, O. P.; Strauss, S. H. *J. Am. Chem. Soc.* **1991**, *113*, 6277−6278.
(100) Hurlburt, P. K.; Rack, J. J.; Dec, S. F.; Anderson, O. P.; Strauss, S. H. *Inorg. Chem.* **1993**, *32*, 373−374.
(101) Hurlburt, P. K.; Rack, J. J.; Luck, J. S.; Dec, S. F.; Webb, J. D.; Anderson, O. P.; Strauss, S. H. *J. Am. Chem. Soc.* **1994**, *116*, 10003−10014.
(102) Willner, H.; Bodenbinder, M.; Bröchler, R.; Hwang, G.; Rettig, S. J.; Trotter, J.; von Ahsen, B.; Westphal, U.; Jonas, V.; Thiel, W.; Aubke, F. *J. Am. Chem. Soc.* **2001**, *123*, 588−602.
(103) Carofiglio, T.; Floriani, C.; Chiesi-Villa, A.; Guastini, C. *Inorg. Chem.* **1989**, *28*, 4417−4419.
(104) Ahlers, W.; Erker, G.; Fröhlich, R. *J. Organomet. Chem.* **1998**, *571*, 83−89.
(105) La Pierre, H. S.; Arnold, J.; Bergman, R. G.; Toste, F. D. *Inorg. Chem.* **2012**, *51*, 13334−13344.
(106) Bendix, J.; Bogevig, A. *Inorg. Chem.* **1998**, *37*, 5992−6001.
(107) Bondi, A. *J. Phys. Chem.* **1964**, *68*, 441−451.
(108) Thalladi, V. R.; Weiss, H.-C.; Bläser, D.; Boese, R.; Nangia, A.; Desiraju, G. R. *J. Am. Chem. Soc.* **1998**, *120*, 8702−8710.
(109) Anthon, C.; Bendix, J.; Schäffer, C. E. *Inorg. Chem.* **2003**, *42*, 4088−4097.
(110) Schäffer, C. E.; Anthon, C.; Bendix, J. *Coord. Chem. Rev.* **2009**, *253*, 575−593.
(111) Boehme, C.; Frenking, G. *Organometallics* **1998**, *17*, 5801−5809.
(112) Deubel, D. V. *Organometallics* **2002**, *21*, 4303−4305.
(113) Abernethy, C. D.; Codd, G. M.; Spicer, M. D.; Taylor, M. K. *J. Am. Chem. Soc.* **2003**, *125*, 1128−1129.
(114) Hu, X.; Tang, Y.; Gantzel, P.; Meyer, K. *Organometallics* **2003**, *22*, 612−614.
(115) Hu, X.; Castro-Rodriguez, I.; Olsen, K.; Meyer, K. *Organometallics* **2004**, *23*, 755−764.
(116) Lauffer, R. B. *Chem. Rev.* **1987**, *87*, 901−927.
(117) Perez, J. M.; Josephson, L.; O'Loughlin, T.; Högemann, D.; Weissleder, R. *Nat. Biotechnol.* **2002**, *20*, 816−820.
(118) Fulmer, G. R.; Miller, A. J. M.; Sherden, N. H.; Gottlieb, H. E.; Nudelman, A.; Stoltz, B. M.; Bercaw, J. E.; Goldberg, K. I. *Organometallics* **2010**, *29*, 2176−2179.

DOI: 10.1021/acs.inorgchem.5b00112
Inorg. Chem. 2015, 54, 3562−3572